Contribution from the Department of Chemistry and
Materials Research Center, Northwestern University, Evanston, Illinois 60201

Synthesis and Characterization of the Bis(diselenolene) Complexes $[M(Se_2C_2(CF_3)_2)_2]^z$ (M = Pt, z = 0, -1, -2; M = Au, z = -1) and Crystal Structure of $[(C_6H_5)_4P][Pt(Se_2C_2(CF_3)_2)_2]$

William B. Heuer, Anne E. True, Paul N. Swepston,[1] and Brian M. Hoffman*

Received April 9, 1987

New metal diselenolene complexes with the formula $[M(Se_2C_2(CF_3)_2)_2]^z$ (M = Pt, z = 0, -1, -2; M = Au, z = -1) have been prepared by the reaction of bis(trifluoromethyl)diselenete, $(CF_3)_2C_2Se_2$, with $(Ph_3P)_2PtCl_2$ and $(Ph_3P)AuCl$, respectively; the previously known Ni and Cu analogues have been similarly obtained. Comparison of electrochemical data for these complexes with those of the corresponding metal bis(dithiolene) complexes indicates that substitution of selenium for sulfur does not dramatically alter the electronic structure. Analysis of ESR spectra of the paramagnetic $[M(Se_2C_2(CF_3)_2)_2]^-$ (M = Ni, Pt) anions indicates that the majority (ca. 70%) of the unpaired spin is located on the four selenium atoms. The neutral complex $[Pt(Se_2C_2(CF_3)_2)_2]$ exhibits an unusual associational equilibrium in solution that has been studied by UV-vis and ^{19}F NMR spectroscopy. The X-ray crystal structure of $[(C_6H_5)_4P][Pt(Se_2C_2(CF_3)_2)_2]$ also is reported; the coordination geometry of Pt is nominally square planar, with interatomic distances reflecting substantial multiple-bond character in the Pt-Se bonds. Crystal data: monoclinic, space group $P2_1/c$, with a = 18.015 (3) Å, b = 14.280 (4) Å, c = 14.627 (4) Å, β = 112.30 (2)°, V = 3481.4 (9) Å^3, and Z = 4.

Introduction

Planar transition-metal bis(dithiolene) complexes[2] have long been viewed as attractive precursors for the synthesis of highly conducting molecular solids ("molecular metals")[3] due to their highly delocalized electronic structure, range of stable oxidation states, and propensity to adopt linear-chain structures in the solid state.[3] Although early efforts to prepare molecular metals based on such complexes met with only limited success,[3d] more recent work[4,5] has yielded a growing family of highly conducting compounds, some of which possess unusual quasi-two- or quasi-three-dimensional structures.

In principle, the selenium analogues of such complexes (metal bis(diselenolenes)) should be better suited to the formation of such extended, multidimensional molecular arrays due to the greater polarizability and larger van der Waals radius of selenium compared to those of sulfur. However, due to the limited number of preparative routes available and the reduced stability of such complexes relative to that of their sulfur-containing analogues, only a few examples of metal bis(diselenolene) complexes have been reported,[6-8] and their solid-state chemistry remains virtually unexplored. In view of this fact, we have prepared and characterized a series of metal bis(diselenolene) complexes of the type

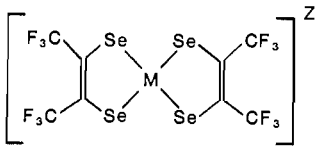

M	Z
Ni	-1, -2
Pt	0, -1, -2
Cu	-1
Au	-1

for use in the synthesis of conductive molecular crystals.[9]

Like their sulfur-containing analogues,[10] such complexes, hereafter abbreviated[11] $[M(tds)_2]$ (tds = [bis(trifluoromethyl)-ethylene]diselenolato), can adopt a range of oxidation states that depends upon the identity of the central metal ion. The complete series of Ni and Cu species indicated above was originally prepared by Davison and Shawl;[6] Wudl and co-workers[8] have subsequently reported an alternate route to the monoanionic Ni complex. We now report the preparation and characterization of the corresponding series of Pt and Au complexes and also describe a new preparation of the Ni complexes. The new complexes have been characterized by ESR, cyclic voltammetry, and, in the case of M = Pt, a single-crystal X-ray structure determination. An unusual associational equilibrium of $[Pt(tds)_2]$ in solution also has been studied by UV-vis and ^{19}F NMR spectroscopy. In general, our results indicate that metal bis(diselenolene) complexes behave similarly to their sulfur-based analogues.

Experimental Section

Starting Materials. Bis(trifluoromethyl)diselenete (I) was prepared by using the method of Davison and Shawl;[6] to prevent dimerization, this material was stored at 77 K until used. Dichlorobis(triphenyl-

(1) Current address: Molecular Structure Corp., College Station, TX.
(2) (a) McCleverty, J. A. *Prog. Inorg. Chem.* **1968**, *10*, 49-221. (b) Burns, R. P.; McAuliffe, C. A. *Adv. Inorg. Chem. Radiochem.* **1979**, *22*, 303-348.
(3) (a) Hatfield, W. E., Ed. *Molecular Metals*; Plenum: New York, 1979. (b) Devreese, J. T., Evrard, R. P., Van Doren, V. E., Eds. *Highly Conducting One-Dimensional Solids*; Plenum: New York, 1979. (c) Miller, J. S., Ed. *Extended Linear Chain Compounds*; Plenum: New York, 1982 (Vol. 1 and 2), 1983 (Vol. 3). (d) Alcacer, L.; Novais, H. In ref 3c, Vol. 3, pp 319-351.
(4) (a) Kato, R.; Mori, T.; Kobayashi, A.; Sasaki, Y.; Kobayashi, H. *Chem. Lett.* **1984**, 1-4. (b) kato, R.; Kobayashi, H.; Kobayashi, A.; Sasaki, Y. *Chem. Lett.* **1985**, 131-134. (c) Kobayashi, H.; Kato, R.; Kobayashi, A.; Sasaki, Y. *Chem. Lett.* **1985**, 191-194. (d) Kobayashi, H.; Kato, R.; Kobayashi, A.; Sasaki, Y. *Chem. Lett. Ibid.* **1985**, 535-538. (e) Underhill, A. E.; Tonge, J. S.; Clemenson, P. I. *Mol. Cryst. Liq. Cryst.* **1985**, *125*, 439-446. (f) Kobayashi, H.; Kato, R.; Mori, T.; Kobayashi, A.; Sasaki, Y.; Saito, G.; Inokuchi, H. *Chem. Lett.* **1985**, 125-134. (g) Kobayashi, A.; Sasaki, Y.; Kato, R.; Kobayashi, H. *Chem. Lett.* **1986**, 387-390.
(5) (a) Brossard, L.; Ribault, M.; Bousseau, M.; Valade, L.; Cassoux, P. *C. R. Acad. Sci.* **1986**, *302*, 205-210. (b) Bousseau, M.; Valade, L.; Legros, J.-P.; Cassoux, P.; Garbauskas, M.; Interrante, L. V. *J. Am. Chem. Soc.* **1986**, *108*, 1908-1916.
(6) (a) Davison, A.; Shawl, E. T. *J. Chem. Soc., Chem. Commun.* **1967**, 670. (b) Davison, A.; Shawl, E. T. *Inorg. Chem.* **1970**, *9*, 1820-1825.
(7) (a) Sandman, D. J.; Stark, J. C.; Acampora, L. A.; Samuelson, L. A.; Allen, G. W.; Jansen, S.; Jones, M. T.; Foxman, B. M. *Mol. Cryst. Liq. Cryst.* **1984**, *107*, 1-17. (b) Sandman, D. J.; Stark, J. C.; Allen, G.; Acampora, L. A.; Jones, M. T.; Jansen, S.; Ashwell, G. J. *Mol. Cryst. Liq. Cryst.* **1985**, *120*, 405-412. (c) Jones, M. T.; Jansen, S.; Sandman, D. J.; Foxman, B. M. *Mol. Cryst. Liq. Cryst.* **1985**, *125*, 429-437.
(8) Wudl, F.; Zellers, E. T.; Cox, S. D. *Inorg. Chem.* **1985**, *24*, 2864-2866.
(9) (a) Heuer, W. B.; Hoffman, B. M. *J. Chem. Soc., Chem. Commun.* **1986**, 174-175. (b) Heuer, W. B.; Squattrito, P. J.; Ibers, J. A.; Hoffman, B. M., manuscript submitted for publication.
(10) (a) Davison, A.; Edelstein, N.; Holm, R. H.; Maki, A. H. *Inorg. Chem.* **1963**, *2*, 1227-1232. (b) Davison, A.; Edelstein, N.; Holm, R. H.; Maki, A. H. *Inorg. Chem.* **1964**, *3*, 814-823. (c) Davison, A.; Howe, D. V.; Shawl, E. T. *Inorg. Chem.* **1967**, *6*, 458-463.
(11) Abbreviations: tds, bis(trifluoromethyl)ethylenediselenolato; tfd, bis-(trifluoromethyl)ethylenedithiolato; edt, ethylene-1,2-dithiolato; dtc, diethyldithiocarbamato; mnt, maleonitriledithiolato.

0020-1669/88/1327-1474$01.50/0

phosphine)platinum(II) and tetrameric (triphenylphosphine)copper(I) iodide were prepared by using published procedures.[12] All other reagents and solvents employed in synthetic procedures were obtained from standard commercial sources and used without further purification.

Synthesis. $[(C_4H_9)_4N][Ni(tds)_2]$. A solution of I (2.92 g, 9.1 mmol) in CH_2Cl_2 (20 mL) was added dropwise to a stirred solution of dicarbonylbis(triphenylphosphine)nickel(0) (2.06 g, 3.2 mmol) in CH_2Cl_2 (50 mL). The reaction mixture was stirred at 25 °C until gas evolution was complete, brought to reflux for 1 h, and then taken to dryness under vacuum; unreacted I was trapped with the use of a liquid-N_2 condenser. The residue was resuspended in 20% aqueous MeOH (25 mL) and cooled to 0 °C to precipitate the triphenylphosphine selenide byproduct, which was removed by filtration. The green filtrate was extracted with *n*-pentane (3 × 50 mL) and decanted into a solution of tetrabutylammonium bromide (1.25 g, 3.88 mmol) in 50% aqueous MeOH (20 mL). The resulting crude precipitate was washed with *n*-pentane to remove residual malodorous impurities before recrystallization from hot aqueous 2-propanol: yield 2.36 g (79%) of green plates; mp 92–93 °C. Anal. Calcd for $C_{24}H_{36}NSe_4F_{12}Ni$: C, 30.62; H, 3.83; N, 1.49; F, 24.24. Found: C, 30.71; H, 3.73; N 1.46; F, 24.56. IR (ν, cm^{-1}): 1518 (C=C str); 1225, 1160, 1136, 1110 (C—F str). UV–vis (λ, nm (log ϵ)): 268 (4.53), 330 (4.93), 394 (3.64), 474 (3.04), 624 (3.15).

$[(C_4H_9)_4]_2[Ni(tds)_2]$. A solution of $[(C_4H_9)_4][Ni(tds)_2]$ (1.50 g, 1.59 mmol) in MeOH (40 mL) was reduced by addition of 85% hydrazine hydrate (0.2 g, 5.3 mmol). The resulting yellow solution was decanted into a solution of tetrabutylammonium bromide (0.75 g, 1.78 mmol) in 50% aqueous MeOH (20 mL); a brown precipitate was isolated by vacuum filtration. The crude product was recrystallized by dissolving the solid in a minimum volume of MeOH at 25 °C and then cooling the solution to 0 °C and slowly adding a solution of tetrabutylammonium bromide in aqueous MeOH. Due to the air sensitivity of the dianion in solution, solvents were deoxygenated by bubbling with N_2 before use, and all operations were performed under a nitrogen atmosphere: yield 1.55 g (82%) of tan needles; mp 134–135 °C. Anal. Calcd for $C_{40}H_{72}N_2Se_4F_{12}Ni$: C, 40.59; H, 6.09; N, 2.37; F, 19.28. Found: C, 40.63; H, 5.99; N, 2.63; F, 18.75. IR (ν, cm^{-1}): 1527 (C=C str); 1226, 1145, 1110 (C—F str). UV–vis (λ, nm (log ϵ)): 334 (4.18), 408 (3.38).

$[Pt(tds)_2]$. Dichlorobis(triphenylphosphine)platinum(II) (0.50 g, 0.63 mmol) was suspended in toluene (200 mL) and briefly brought to reflux. The temperature was then reduced to 90 °C, and a solution of I (0.80 g, 2.5 mmol) in toluene (20 mL) was added. The mixture was stirred at 90 °C for 6 h, over which time it acquired a deep blue color; when the mixture was cooled, however, a muddy red color was observed. The reaction mixture was taken to dryness under vacuum, with use of a liquid-N_2 trap to collect unreacted I. The residual oily solids were suspended in a minimum volume of CH_2Cl_2 and chromatographed on silica gel (Woelm TSC grade, activity III) with CH_2Cl_2 as the eluent. After the unreacted I was washed off the column as a yellow band, the solvent polarity was increased by adding ethyl acetate and finally acetone. The desired product $[Pt(tds)_2]$ was eluted with 2:1 ethyl acetate/acetone as a broad, red-brown band, which was collected and taken to dryness under vacuum. The dark oily residue was further purified by repeating the chromatographic procedures described above; this time, however, the CH_2Cl_2 eluent washed a continuous stream of faint blue coloration out of the dark band at the head of the column. The bulk of the product was eluted with ethyl acetate/acetone (1:1) and recovered as a red oil, which solidified upon drying under vacuum; yield 0.48 g (90%).

Efforts to crystallize the product from solution were unsuccessful, as were attempts to sublime it onto a cold finger under vacuum. Acceptable elemental analyses could not be obtained due to residual solvent in the dried oil; the IR and mass spectra, however, support the proposed formulation as the neutral bis-substituted complex. IR (ν, cm^{-1}): 1555 (C=C str); 1230, 1180, 1160 (C—F str). MS (*m/e*, amu): 836 (M^+), 674 ($M^+ - C_4F_6$), 511 ($M^+ - C_8F_{12}$), 482 ($C_8Se_2F_{12}$, fragmentation product), 319 ($C_4Se_2F_6$, free ligand).

$[(C_6H_5)_4P][Pt(tds)_2]$. An acetone solution (150 mL) containing $[Pt(tds)_2]$ (0.5 g, 0.60 mmol) and $SnCl_2 \cdot 2H_2O$ (0.13 g, 0.60 mmol) was refluxed under N_2 for 2 h. The mixture was then cooled to room temperature, and a solution of tetraphenylphosphonium bromide (0.34 g, 0.8 mmol) in 50% aqueous acetone (20 mL) was added; upon slow evaporation, the solution deposited long black needle crystals. These were isolated and redissolved in a minimum volume of CH_2Cl_2, and the solution was filtered to remove the insoluble Sn residues. The filtrate was taken to dryness, and the residue was recrystallized two times from 20% aqueous acetone: yield 0.42 g (60%) of black needles; mp 190–192 °C. Anal. Calcd for $C_{32}H_{20}PSe_4F_{12}Pt$: C, 32.71; H, 1.70; F, 19.42. Found: C, 32.75; H, 1.70; F, 19.97. IR (ν, cm^{-1}): 1590 (C=C str); 1215, 1159, 1125 (C—F str). UV–vis (λ, nm (log ϵ)): 236 (4.88), 264 (4.41), 270 (4.40), 294 (4.11), 458 (3.30), 576 (3.30), 646 (3.15).

$[(C_6H_5)_4P]_2[Pt(tds)_2]$. A solution of $[Pt(tds)_2]$ (0.5 g, 0.60 mmol) in 70% aqueous EtOH (30 mL) was treated with 80% aqueous N_2H_4 (0.1 g, 2.6 mmol) and the mixture was then decanted into a solution of tetraphenylphosphonium bromide (0.63 g, 1.5 mmol) in aqueous EtOH (10 mL). The volume of the resulting mixture was reduced by warming gently under partial vacuum until solids began to form; the flask was then sealed and set aside to cool. The crystalline product was isolated by suction filtration: yield 0.59 g (65%) of orange plates; mp 263–265 °C dec. IR (ν, cm^{-1}): 1585 (C=C str); 1225, 1140, 1105 (C—F str). UV–vis (λ, nm (log ϵ)): 394 (3.43), 412 (3.40), 490 (2.63).

$[(C_6H_5)_4P][Cu(tds)_2]$. This complex was prepared by using a variation of the procedure reported by Davison and Shawl.[6b] (Triphenylphosphine)copper(I) iodide (0.2 g, 0.11 mmol) was suspended in benzene (20 mL), and the mixture was stirred at 25 °C for 1 h. A solution of I (0.5 g, 1.56 mmol) in benzene (5 mL) was added, and the mixture was stirred at 25 °C for 4 h. It was then taken to dryness under vacuum with the use of a liquid-N_2 trap, and the residue was resuspended in 70% aqueous EtOH. The resulting solution was filtered to remove triphenylphosphine selenide and extracted with *n*-pentane (3 × 50 mL) before being decanted into a solution of tetraphenylphosphonium bromide (0.2 g, 0.48 mmol) in aqueous EtOH (10 mL). The mixture was allowed to slowly evaporate, and the deposited solids were collected and recrystallized from hot aqueous 2-propanol: yield 0.20 g (43%) of maroon needles; mp 150–152 °C. Anal. Calcd for $C_{32}H_{20}PSe_4F_{12}Cu$: C, 36.84; H, 1.92; F, 21.87. Found: C, 36.59; H, 1.87; F, 22.12. IR (ν, cm^{-1}): 1579 (C=C str); 1240, 1158, 1130 (C—F str). UV–vis (λ, nm (log ϵ)): 230 (4.41), 270 (4.11), 276 (4.08), 292 (3.88), 405 (4.08), 536 (3.08).

$[(C_4H_9)_4N][Au(tds)_2]$. Chloro(triphenylphosphine)gold(I) (0.2 g, 0.40 mmol) was dissolved in benzene (20 mL), and a solution of I (0.40 g, 1.25 mmol) in benzene (5 mL) was added. The mixture was stirred at 25 °C for 30 min and then gradually heated to reflux; after 1 h of refluxing, the solvent was removed under vacuum with the use of a liquid-N_2 trap. The oily residue was swirled with several small (ca. 10 mL) volumes of *n*-pentane, which were decanted and set aside. The product in the flask crystallized during this procedure, and more crystals were recovered from the concentrated pentane washings. These solids were combined and resuspended in 2-propanol; the resulting green solution was filtered to remove unreacted chloro(triphenylphosphine)gold(I), and the filtrate was briefly heated to boiling after the addition of some H_2O. The hot solution was decanted into a solution of tetrabutylammonium bromide (0.15 g, 0.46 mmol), and the mixture was set aside to cool. The resulting green crystals were recrystallized two times by using the same procedure: yield 0.23 g (53%) of lime green plates; mp 90–91 °C. Anal. Calcd for $C_{24}H_{36}NSe_4F_{12}Au$: C, 26.70; H, 3.34; N, 1.30; F, 21.13. Found: C, 26.76; H, 3.32; N, 1.28; F, 20.65. IR (ν, cm^{-1}): 1558 (C=C str); 1230, 1158, 1135 (C—F str). UV–vis (λ, nm (log ϵ)): 240 (4.51), 254 (4.51), 306 (4.36).

Methods. UV–vis spectra were recorded on a Hewlett-Packard Model 8451A photodiode array spectrophotometer. Spectra normally were obtained of tetrahydrofuran (Aldrich, Gold Label) solutions; studies of the concentration and temperature dependence of the spectrum of $[Pt(tds)_2]$ used freshly distilled toluene (Aldrich, Gold Label). The sample temperature was regulated within ±0.5 °C with a thermostatable cell holder connected to a constant-temperature bath; the temperature was measured with a copper–constantan thermocouple in contact with the sample. IR spectra were recorded on a Perkin-Elmer Model 283 spectrophotometer. Mass spectra were obtained on a Hewlett-Packard Model 5985 GC/MS system using 70-eV electron-impact ionization. ESR spectra were recorded at X-band (ca. 9 GHz) with a highly modified Varian Model E-4 spectrometer with 100-kHz field modulation. The microwave frequency was measured with a Hewlett-Packard Model X532B frequency meter, and the magnetic field was calibrated with DPPH (2,2-diphenyl-1-picrylhydrazyl; $g = 2.0036$) as the external standard. Low-temperature (77 K) spectra were obtained by immersing the sample in liquid N_2. Computer simulations of observed spectra were performed on a Harris 1000 computer with the program QPOW.[13] ^{77}Se and ^{19}F NMR spectra were recorded on a Varian XLA-400 spectrometer operating at frequencies of 76 and 376 MHz, respectively. ^{77}Se chemical shifts were referenced to external diphenyl diselenide, while ^{19}F shifts were referenced to internal $CFCl_3$. Cyclic voltammetry was performed

(12) (a) Malatesta, L.; Cariello, C. *J. Chem. Soc.* **1958**, 2323–2328. (b) Costa, G.; Reisenhofer, E.; Stefani, L. *J. Inorg. Nucl. Chem.* **1965**, *27*, 2581–2584.

(13) (a) Belford, R. L.; Nilges, M. J. "Computer Simulation of Powder Spectra", paper presented at the EPR Symposium, 21st Rocky Mountain Conference, Denver, CO, August, 1979. (b) Nilges, M. J. Ph.D. Thesis, University of Illinois, 1981. Altman, T. E. Ph.D. Thesis, University of Illinois, 1981. Maurice, A. M. Ph.D. Thesis, University of Illinois, 1982. Duliba, E. P. Ph.D. Thesis, University of Illinois 1983.

Table I. Summary of Crystal Data and Intensity Collection Parameters

formula	$C_{32}H_{20}PF_{12}Se_4Pt$
fw	1173.9
cryst size, mm	0.3 × 0.05 × 0.09
space group	$P2_1/c$ (No. 14)
cryst syst	monoclinic
a, Å	18.015 (3)
b, Å	14.280 (4)
c, Å	14.627 (4)
β, deg	112.30 (2)
V, Å^3	3481.4 (9)
Z	4
ρ(calcd), g/cm^3	2.241
T, K	148
λ(Mo Kα), Å	0.71073
μ(Mo Kα), cm^{-1}	83.45
2θ range, deg	$2 \le 2\theta \le 48$
scan speed, ω scale, deg/min	1.03–2.35
scan mode	$\omega/2\theta$
scan width, deg	$\omega = 0.7 \pm 0.35 \tan\theta$
no. of reflns measd	$\pm h,+k,+l$
no. of reflns collected	5448
no. of unique rflns with $I < 2\sigma(I)$	2857
no. of params	416
transmission factors	0.868–1.000
R, R_w[a]	0.0510, 0.0567
weighting scheme	$w = 1/\sigma^2(\lvert F_o\rvert)$

[a] $R = \sum\lvert\lvert F_o\rvert - \lvert F_c\rvert\rvert/\sum\lvert F_o\rvert$; $R_w = \{\sum w(\lvert F_o\rvert - \lvert F_c\rvert)^2/\sum\lvert F_o\rvert^2\}^{1/2}$

with a BAS Model CV-27 potentiostat and a Houston Instruments Model 2000 x-y recorder. Acetonitrile (Aldrich, Gold Label) was distilled under N_2 from CaH_2 immediately before use. Tetrabutylammonium tetrafluoroborate was prepared by standard procedures,[14] recrystallized three times from ethyl acetate/*n*-pentane, and dried in vacuo at 100 °C. Solutions were 0.1 M in supporting electrolyte and ca. 0.1 mM in metal complex. The Pt working electrode was cleaned just prior to use by potential cycling in 0.1 M H_2SO_4. Potentials were recorded vs a nonaqueous Ag/Ag^+ reference (+0.338 V vs SCE).

X-ray Crystal Structure of $[(C_6H_5)_4P][Pt(tds)_2]$. Crystals of $[(C_6H_5)_4P][Pt(tds)_2]$ suitable for X-ray diffraction measurements were obtained as black needles by slow evaporation of an aqueous acetone solution. A crystal with approximate dimensions 0.3 mm × 0.05 mm × 0.09 mm was mounted on a glass fiber and placed in the N_2 cold stream (T = 148 K) on an Enraf-Nonius CAD4 diffractometer. Pertinent crystal, data collection, and refinement parameters are summarized in Table I. All crystallographic computations were performed on a VAX 11/730 computer with the SDP crystallographic software package.[15] Data were corrected for Lorentz and polarization effects. An empirical absorption correction was calculated on the basis of ψ-scan data with the program EAC.[15] Atomic scattering and anomalous dispersion factors for the non-hydrogen atoms were taken from Cromer and Waber.[16]

Lattice parameters were refined by least squares on the basis of 25 well-centered reflections ($25° \le 2\theta \le 28°$) measured with graphite-monochromated Mo Kα radiation. Data collection parameters are listed in Table I. The intensities of six standard reflections were measured every 100 min, with no significant variations in intensity during 48 h of data collection.

The initial coordinates of the platinum atom were determined from an interpretation of the Patterson function. All remaining non-hydrogen atoms were located and refined through an alternating series of least-squares cycles and difference Fourier maps. Hydrogen atoms were not refined but were included in the structure factor calculations as fixed contributors to the scattering at a distance of 0.95 Å from the bonded carbon atoms. Some of the atoms were refined with isotropic temperature factors because their temperature factors became nonpositive definite upon anisotropic refinement.

The final cycle of full-matrix least-squares refinement involved 416 variables and 2857 unique reflections with $I > 2\sigma(I)$. The final residuals are $R(F) = 0.0510$ and $R_w(F) = 0.0567$, and the error in an observation of unit weight is 1.1763. The final difference map showed a maximum peak height of 2.779 e/Å^3 located 1.05 Å from the platinum atom. Final positional and equivalent isotropic thermal parameters are given in Table II. Listings of idealized hydrogen atom positions, temperature factors, and observed and calculated structure factors are available as supplementary material.

Table II. Positional and Equivalent Isotropic Thermal Parameters[a] of All Non-Hydrogen Atoms for $[(C_6H_5)_4P][Pt(tds)_2]$

atom	x	y	z	B_{eq}, Å^2
Pt	0.2876 (4)	0.14250 (5)	−0.12135 (5)	1.31 (1)
Se(1)	0.3398 (1)	0.2664 (1)	−0.1855 (1)	1.58 (4)
Se(2)	0.4186 (1)	0.1049 (1)	−0.0087 (1)	1.69 (4)
Se(3)	0.2324 (1)	0.0111 (1)	−0.0706 (1)	1.82 (4)
Se(4)	0.1574 (1)	0.1932 (1)	−0.2232 (1)	1.70 (4)
P	0.2457 (3)	0.4632 (4)	0.0340 (3)	1.5 (1)
F(1)	0.4576 (6)	0.3700 (9)	−0.2266 (8)	3.2 (3)
F(2)	0.5083 (7)	0.4113 (8)	−0.0743 (8)	3.2 (3)
F(3)	0.5688 (6)	0.3111 (8)	−0.1285 (8)	2.9 (3)
F(4)	0.6043 (6)	0.2726 (8)	0.0578 (8)	2.8 (3)
F(5)	0.6119 (6)	0.1456 (8)	−0.0182 (8)	2.8 (3)
F(6)	0.5823 (6)	0.1388 (8)	0.1087 (7)	2.6 (3)
F(7)	0.1113 (6)	−0.1284 (8)	−0.0920 (9)	3.9 (3)
F(8)	0.0066 (7)	−0.0706 (9)	−0.2005 (9)	4.0 (3)
F(9)	0.0450 (8)	−0.024 (1)	−0.0501 (9)	5.3 (3)
F(10)	−0.0294 (7)	0.0695 (9)	−0.3356 (8)	3.7 (3)
F(11)	−0.0403 (6)	0.1067 (8)	−0.1996 (8)	2.9 (3)
F(12)	−0.0104 (7)	0.2114 (8)	−0.286 (1)	4.1 (4)
C(1)[b]	0.450 (1)	0.262 (1)	−0.111 (1)	1.8 (4)
C(2)[b]	0.4812 (9)	0.198 (1)	−0.036 (1)	1.3 (4)
C(3)	0.120 (1)	0.026 (1)	−0.140 (1)	2.3 (5)
C(4)	0.092 (1)	0.102 (1)	−0.199 (1)	1.9 (4)
C(5)	0.497 (1)	0.337 (1)	−0.136 (1)	2.3 (5)
C(6)	0.570 (1)	0.188 (1)	0.028 (1)	2.2 (5)
C(7)	0.072 (1)	−0.046 (1)	−0.118 (2)	3.3 (6)
C(8)	0.003 (1)	0.124 (1)	−0.256 (1)	2.0 (4)
C(9)[b]	0.218 (1)	0.570 (1)	0.076 (1)	1.6 (4)
C(10)	0.191 (1)	0.570 (1)	0.156 (1)	2.0 (4)
C(11)	0.180 (1)	0.652 (1)	0.195 (1)	3.0 (5)
C(12)	0.192 (1)	0.741 (1)	0.157 (2)	3.6 (6)
C(13)	0.215 (1)	0.739 (1)	0.076 (2)	3.1 (5)
C(14)[b]	0.228 (1)	0.656 (1)	0.037 (1)	2.3 (4)
C(15)	0.2495 (9)	0.480 (1)	−0.086 (1)	1.7 (4)
C(16)	0.315 (1)	0.518 (1)	−0.098 (1)	1.8 (4)
C(17)	0.320 (1)	0.533 (1)	−0.188 (1)	2.5 (5)
C(18)	0.254 (1)	0.505 (2)	−0.273 (1)	2.7 (5)
C(19)	0.186 (1)	0.466 (1)	−0.262 (1)	2.2 (4)
C(20)[b]	0.183 (1)	0.451 (1)	−0.170 (1)	1.9 (4)
C(21)[b]	0.345 (1)	0.434 (1)	0.117 (1)	1.5 (4)
C(22)	0.380 (1)	0.478 (1)	0.207 (1)	1.6 (4)
C(23)	0.459 (1)	0.455 (1)	0.269 (1)	2.1 (4)
C(24)	0.500 (1)	0.386 (2)	0.246 (1)	2.8 (5)
C(25)	0.464 (1)	0.338 (1)	0.155 (1)	2.6 (5)
C(26)	0.387 (1)	0.361 (1)	0.092 (1)	2.6 (5)
C(27)[b]	0.174 (1)	0.375 (1)	0.029 (1)	1.8 (4)
C(28)	0.093 (1)	0.402 (1)	0.001 (1)	2.5 (5)
C(29)	0.037 (1)	0.334 (1)	−0.008 (1)	2.6 (5)
C(30)	0.059 (1)	0.238 (2)	0.007 (1)	2.9 (5)
C(31)	0.138 (1)	0.214 (1)	0.031 (1)	2.8 (5)
C(32)	0.194 (1)	0.281 (1)	0.043 (1)	1.9 (4)

[a] Equivalent isotropic thermal parameter defined as $^4/_3[a^2B(1,1) + b^2(2,2) + c^2B(3,3) + ab(\cos\gamma)B(1,2) + ac(\cos\beta)B(1,3) + bc(\cos\alpha)B(2,3)]$. [b] Refined with isotropic thermal parameters.

Results and Discussion

Synthesis of $M(tds)_2$ Complexes. Heterocycles of the type

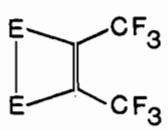

E = S, Se

form metal complexes by oxidative addition to low-valent metal centers. For example, bis(trifluoromethyl)dithiete (I, E = S) reacts cleanly with zerovalent metal carbonyl complexes:[10a,b]

$$M(CO)_x + nS_2C_2(CF_3)_2 \rightarrow M(S_2C_2(CF_3)_2)_n + xCO(g)\uparrow \quad (1)$$

$Ni(CO)_4$, $Fe(CO)_5$, and $Co_2(CO)_8$ react to form bis chelate

(14) Sawyer, D. T.; Roberts, J. L. *Experimental Electrochemistry for Chemists*; Wiley: New York, 1974; p 212.
(15) *Structure Determination Package*; B. A. Frenz and Associates: College Station, TX (Enraf-Nonius: Delft, Holland), 1982.
(16) Cromer, D. T.; Waber, J. T. *International Tables for X-ray Crystallography*; Kynoch: Birmingham, England, 1974.

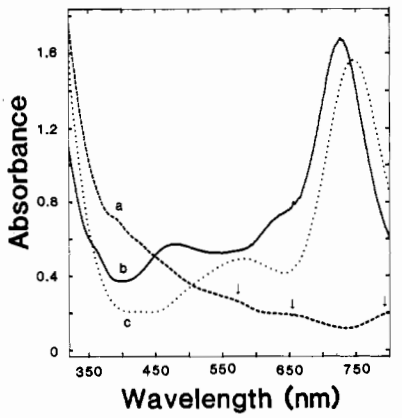

Figure 1. Visible absorption spectra: (a) $[Pt(tds)_2]$ in acetone, ambient temperature; (b) $[Pt(tds)_2]$ in toluene after heating to ~80 °C and recooling to ambient temperature; (c) $[Ni(tfd)_2]$ in toluene. Arrows indicate features due to traces of $[Pt(tds)_2]^-$ resulting from reduction by solvent.

complexes, while with $Mo(CO)_6$ and $W(CO)_6$, tris chelate complexes are obtained; in each case, product formation is favored by the evolution of CO gas. Complexes of metals that do not form simple carbonyls can be prepared by starting with the corresponding halo(triphenylphosphine)metal complexes:[10c]

$$(Ph_3P)_aMX_b + \text{excess } S_2C_2(CF_3)_2 \rightarrow M(S_2C_2(CF_3)_2)_n + Ph_3PSe + \text{organic byproducts} \quad (2)$$

$(Ph_3P)_2PdCl_2$, $(Ph_3P)_2PtCl_2$, $(Ph_3P)CuI$, and $(Ph_3P)AuCl$ all yield bis(planar ligand) complexes ($n = 2$) by this method.

An important difference between reactions 1 and 2 is the absence of a gaseous product in the latter case; instead, the method takes advantage of the susceptibility of phosphines toward oxidation[17] to drive the reaction. A three- to fourfold molar excess of the heterocycle must be used, some of which ultimately reacts irreversibly with triphenylphosphine to give triphenylphosphine sulfide (or selenide) and perfluoromethylated organochalcogen side products.

Although the reactivity of the analogous selenium heterocycle (bis(trifluoromethyl)diselenete (I, E = Se) with metal carbonyl complexes has been investigated, the preparation by Davison and Shawl of $[Cu(tds)_2]^-$ is the only example of the corresponding reaction with a halo(triphenylphosphine)metal complex. This synthesis has been reproduced here, with minor modifications. In addition, this work extends the sulfur/selenium analogy with the corresponding preparation of the Ni, Pt, and Au complexes. In general, we find that the chemistry of the selenium-containing complexes follows closely that of the sulfur analogues.

Associational Equilibrium of $[Pt(tds)_2]$. Visible absorption spectra of $[Pt(tds)_2]$ solutions exhibit solvent, concentration, and temperature dependences that indicate that the complex associates in solution. In polar solvents such as acetone or methanol, red solutions are obtained that have a strong UV absorption at 266 nm that tails into the visible region (Figure 1); the character of the spectrum in this case does not change upon heating. In contrast, with less polar solvents such as toluene or chloroform, warming the solution above room temperature induces a dramatic change of color from red to blue. When cooled back to room temperature, the solution slowly reverts back to its original red color at a rate that depends upon both solvent and concentration: at higher concentrations and/or in more polar solvents (i.e., chloroform vs toluene), the red color returns more quickly. The visible absorption spectrum of the deep blue toluene solution obtained upon heating is dominated by a strong band centered at 724 nm. Such low-energy absorptions are characteristic of neutral metal bis(dithiolene) complexes;[18] indeed, as shown in Figure 1, the visible spectrum of the blue $[Pt(tds)_2]$ solution is quite similar to that of $[Ni(tfd)_2]$, (tfd = bis(trifluoromethyl)-ethylenedithiolato). We infer from this comparison that the blue color arises from the monomeric $[Pt(tds)_2]$ species and the red color is due to an associated form.

The temperature dependence of the visible absorption spectrum for a 0.25 mM solution of $[Pt(tds)_2]$ in toluene is shown in Figure 2. Between −10 and +50 °C, there is an isosbestic point at 598 nm, indicating that only two chromophoric species are present over this temperature range; this is suggestive of a monomer–dimer equilibrium:

$$2[Pt(tds)_2] \overset{K}{\rightleftharpoons} [Pt(tds)_2]_2$$

Thus, for the monomer we assign $\lambda_{max} = 724$ nm, while the dimer species has two absorbance maxima at 470 and 362 nm. At temperatures below −10 °C, deviations from isosbestic behavior

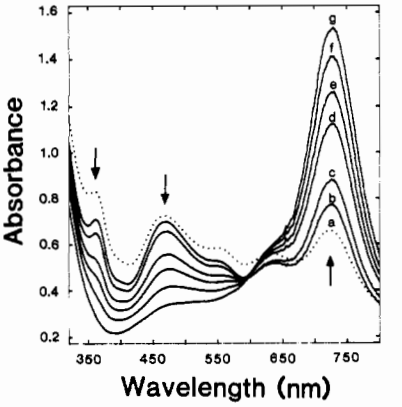

Figure 2. Temperature dependence of the visible absorption spectrum of $[Pt(tds)_2]$, 0.25 mM in toluene: (a) −14.4 °C; (b) −8.9 °C; (c) −3.4 °C; (d) 10.5 °C; (e) 18.0 °C; (f) 29.9 °C; (g) 48.3 °C. Arrows indicate spectral changes observed upon heating.

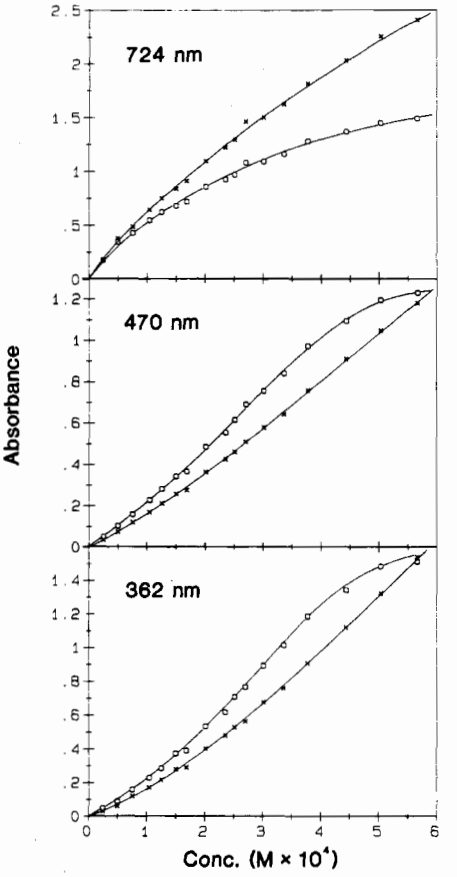

Figure 3. Concentration dependence of the absorbance of $[Pt(tds)_2]$ in toluene at 362, 470, and 724 nm; (○) 25 °C; (×) 5 °C.

(17) Corbridge, D. E. C. *Phosphorus—An Outline of its Chemistry, Biochemistry and Technology*; Elsevier: Amsterdam, 1978; p 155.
(18) Schrauzer, G. N.; Mayweg, V. P. *J. Am. Chem. Soc.* **1965**, *87*, 1483–1489.

are observed, indicating the formation of higher oligomers. We infer from this behavior that the red color exhibited by $[Pt(tds)_2]$ in polar solvents corresponds to the oligomerized species.

The concentration dependence of the absorbance for the equilibrium mixture in toluene was studied at 25 and 5 °C (Figure 3). The observed deviations from Beer's law at 25 °C are indicative of associational behavior; the deviations are more pronounced at 5 °C, reflecting a shift in the equilibrium toward the associated form(s) at lower temperatures. In principle, it is possible to determine the equilibrium constant for the dimerization of $[Pt(tds)_2]$ in toluene solution from the concentration dependence of its optical spectrum. The analysis is complicated by the overlapping absorption spectra of the monomer and dimer species. Also, it is not possible to prepare solutions containing pure monomer or dimer, and therefore their molar extinction coefficients cannot be obtained directly. Boyd and Phillips[19] have described a procedure by which both the value of the equilibrium constant, K, and the extinction coefficients of the monomer and dimer species can be determined in such cases. It relies on extrapolations from self-consistent fits of the concentration dependence of the absorbance at λ_{max}(monomer) and λ_{max}(dimer). An ideal monomer–dimer equilibrium is assumed, and for accuracy this assumption must remain valid over an appreciable range of concentrations.

Application of this method using the absorbances at 724 and 470 nm for the full range of concentrations (0.025–0.6 mM) of $[Pt(tds)_2]$ in toluene at 25 °C failed to yield a fully self-consistent fit, presumably because of the formation of oligomers at the higher concentrations. Nonetheless, our results suggest the following rough estimates: $K \approx 1000$ at 25 °C, $\epsilon_1^M \approx 7500$, $\epsilon_1^D \approx 100$, $\epsilon_2^M \approx 1300$, $\epsilon_2^D \approx 6200$. Here the superscripts M and D designate the extinction coefficients of the monomer and dimer, while the subscripts 1 and 2 refer to λ_{max}(monomer) = 724 nm and λ_{max}(dimer) = 470 nm, respectively. Efforts to improve the fit by using only data at concentrations of less than 0.3 mM, where oligomerization is presumed to be less important, were unsuccessful because the limited range of concentrations introduces an unacceptable level of error into the requisite extrapolation.

It is of interest to consider the possible modes of association for complexes of this type. Because $[Pt(tds)_2]$ is formally a Pt(IV) complex, and Pt(IV) typically exhibits octahedral coordination,[20] it is likely that the solution structure of the associated species involves axial coordination of the central metal ion. Three possible dimer structures that fulfill this requirement are

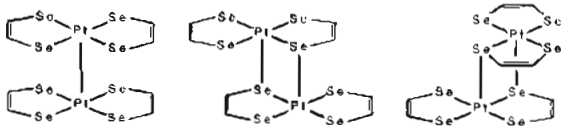

i ii iii

Dimeric structures of types i and ii have previously been found for several neutral metal bis(dithiolene) complexes of the nickel triad. Complexes of the type $[M(edt)_2]$ (edt = ethylene-1,2-dithiolato; M = Pd, Pt) are monomeric in solution but form eclipsed, type i M–M-bonded dimers in the solid state.[21] In contrast, the mixed-ligand compound $[Ni(dtc)(tfd)]_2$ (dtc = diethyldithiocarbamate) exhibits a centrosymmetric type ii structure in which the M–S bonding is mediated by the tfd ligands;[22] here, the dimer structure is apparently preserved in solution. Although no corresponding examples of type iii M–S-bonded structures have been reported, this mode of association might nonetheless be important in $[Pt(tds)_2]$ solutions. In fact, comparison of the type ii and iii structures suggests that the latter configuration is sterically less

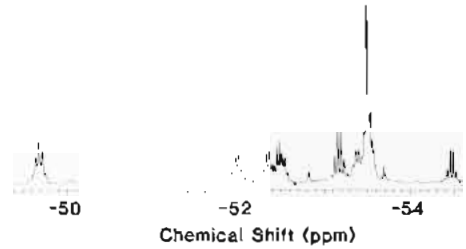

Figure 4. ^{19}F NMR spectrum (376 MHz) of an approximately saturated acetone solution of $[Pt(tds)_2]$. Chemical shifts are referenced to internal $CFCl_3$ (0 ppm). Instrument parameters: spectral width 6631.3 Hz; acquisition time 2.258 s; pulse width 5.0 μs; delay 4.000 s; number of transients 128.

demanding. While steric effects are probably not a dominant factor in determining the structure of the isolated $[Pt(tds)_2]$ dimers, which can presumably distort to minimize repulsions between the CF_3 substituents, they may play a significant role in the formation of oligomeric species, where the possibility of such distortions would be more limited.

Efforts to determine the solution structure of the associated form of $[Pt(tds)_2]$ were made by using NMR spectroscopy. Unfortunately, direct observation of the discrete monomer and dimer species is precluded because they exist only at very low concentrations; however, spectra of the oligomeric form are readily obtained. For example, the ^{19}F NMR spectrum of $[Pt(tds)_2]$ in acetone solution (Figure 4) consists of a series of multiplets with chemical shifts in the range −49 to −55 ppm vs $CFCl_3$. In contrast, the analogous (and presumably monomeric) neutral bis(dithiolene) complex $[Pt(tfd)_2]$ in CH_2Cl_2 solution exhibits a single ^{19}F resonance at −57.5 ppm.[10b,23] This comparison confirms that the multiple resonances in the $[Pt(tds)_2]$ spectrum indeed reflect the formation of oligomers in acetone solution.

Although the complexity of the $[Pt(tds)_2]$ spectrum precludes a detailed analysis, some qualitative observations can nonetheless be made. The quartet splittings exhibited by some of the resonances are characteristic of spin coupling between magnetically inequivalent pairs of CF_3 groups. The apparent lack of symmetry in the disposition of the individual multiplets, and their comparable intensities (the large peak at −53.5 ppm excepted) furthermore argue against the possibility that some of these resonances arise from spin coupling between ^{19}F and ^{77}Se ($I = {}^1/_2$, natural abundance 7.58%) or ^{195}Pt ($I = {}^1/_2$, natural abundance 33.8%). Indeed the ^{77}Se NMR spectrum of the corresponding $[Pt(tds)_2]^{2-}$ ion indicates that the $^{77}Se\{^{19}F\}$ couplings are quite small (≤25 Hz). Thus, it appears that each multiplet of the $[Pt(tds)_2]$ spectrum corresponds to a magnetically distinct type of CF_3 group in the oligomer structure.

Consideration of the dissimilar structural characters of hypothetical Pt–Pt- and Pt–Se-bonded $[Pt(tds)_2]_n$ oligomers suggests that the latter might better account for the complex nature of the ^{19}F NMR spectrum. In a Pt–Pt-bonded oligomer, the CF_3 groups of adjacent molecules all lie on the periphery and therefore occupy similar environments. In contrast, in Pt–Se-bonded oligomers the CF_3 groups would be found in a variety of different environments. This is best illustrated by observing that there are four distinct ways to add a third molecule to either of the Pt–Se bonded dimers ii or iii. Each of the resulting configurations exhibits unique environments for some of the CF_3 substituents; in some cases, individual CF_3 groups lie above and/or below the chelate ring(s) of neighboring $[Pt(tds)_2]$ molecules within the chain, while in others, they are well removed from perturbations by ring currents.[23b] A randomly assembled Pt–Se-bonded oligomer would possess a statistical distribution of each type of environment. Thus, the ^{19}F NMR spectrum of such an oligomer would be expected to exhibit a range of chemical shifts for the CF_3 resonances, in

(19) Boyd, R. H.; Phillips, W. D. *J. Chem. Phys.* **1965**, *43*, 2927–2929.
(20) Cotton, F. A.; Wilkinson, G. *Advanced Inorganic Chemistry*; 4th ed.; Wiley-Interscience: New York, 1980; p 958.
(21) (a) Browall, K. W.; Interrante, L. V.; Kasper, J. S. *J. Am. Chem. Soc.* **1971**, *93*, 6289–6290. (b) Browall, K. W.; Bursh, T.; Interrante, L. V.; Kasper, J. S. *Inorg. Chem.* **1972**, *11*, 1800–1806.
(22) Hermann, A.; Wing, R. M. *Inorg. Chem.* **1972**, *11*, 1415–1420.
(23) (a) The spectrum reported in ref 10b was obtained at a frequency of 40 MHz. (b) Boyde, S.; Garner, C. D.; Joule, J. A.; Rowe, D. J. *J. Chem. Soc., Chem. Commun.* **1987**, 800–801.

Table III. Electrochemistry of $M(tds)_2$ and $M(tfd)_2$ Complexes[a]

M	ligands	couple	$E_{1/2}$, V[b]	ΔE_p, mV	ref
Ni	tds	−1,−2	−0.16	100	*h*
		0,−1	+0.84	*c*	
	tfd	−1,−2	−0.12[e]		10a
		0,−1	+1.00[e]		
Pt	tds	−1,−2	−0.13	100	*h*
		0,−1	+0.74[d]	100[d]	
	tfd	−1,−2	−0.27[e]		10b
		0,−1	+0.82[e]		
Cu	tds	−1,−2	−0.42	80	*h*
		0,−1	+0.94	*c*	
	tfd	−1,−2	−0.01[e]		10c
		0,−1[f]			
Au	tds	−1,−2	−1.10	120	*h*
		0,−1	+1.04	*c*	
	tfd	−1,−2[g]			10c
		0,−1	+1.20[e]		

[a] Conditions: CH_3CN, 0.1 M $[(C_4H_9)_4N][ClO_4]$, stationary Pt working electrode. [b] Volts vs SCE reference. [c] Irreversible at all scan rates. [d] Scan rate dependent (see text). [e] Conditions: CH_3CN, 0.05 M $[(C_3H_7)_4N][ClO_4]$, rotating Pt working electrode. [f] Not reported. [g] No wave found in range 0 to −1.5 V vs SCE. [h] This work.

accord with the experimental result.

Electrochemistry of $M(tds)_2$ Complexes. The results of cyclic voltammetry measurements on the $[M(tds)_2]$ (M = Ni, Pt, Cu, Au) complexes are summarized in Table III, along with literature values for the analogous metal bis(dithiolene) complexes. The $E_{1/2}$ values for corresponding sulfur and selenium complexes are similar, which indicates that the substitution of selenium for sulfur does not dramatically alter the electronic structure. As expected, however, the $[M(tds)_2]$ complexes in general are more easily oxidized than their $[M(tfd)_2]$ counterparts, in accord with the reduced electronegativity of selenium relative to that of sulfur. The single exception to this trend is the $[Pt(tds)_2]^z$ ($z = -1/-2$) couple, which has an $E_{1/2}$ value ca. 15 mV more positive than that of the corresponding $[Pt(tfd)_2]$ couple; the reason for this anomalous result is not clear at present.

The observed dependence of the $[Pt(tds)_2]^z$ ($z = 0/-1$) wave upon the scan rate also is of interest. At slow scan rates, the oxidation of the monoanion is completely irreversible, with no rereduction wave upon scan reversal. However, as the scan rate is increased, a cathodic current peak begins to appear and the wave looks more reversible. These observations may be related to the observed association of the neutral Pt complex in polar media; at slow scan rates, the $[Pt(tds)_2]$ molecules generated at the working electrode surface form dimers and/or oligomers rapidly compared to the scan rate; these associated species apparently are rereduced over a relatively broad potential range, effectively smearing the cathodic wave out into the background current. However, at high sweep rates, comparable to the rate of molecular association, some monomeric $[Pt(tds)_2]$ molecules remain at the electrode surface and contribute to the cathodic current. Preliminary results suggest that this effect can be enhanced by using a less polar solvent (e.g., CH_2Cl_2) and/or reducing the electrolyte concentration.

ESR Spectra of $M(tds)_2$ Complexes. Solution ESR spectra of the paramagnetic $[M(tds)_2]^-$ (M = Ni, Pt) ions were obtained at both room temperature and 77 K. At room temperature, toluene–acetone (1:1) solutions of these complexes yield broad, isotropic resonances with $\langle g \rangle_{iso} = 2.108$ (M = Ni) and 2.073 (M = Pt); when frozen at 77 K, the same solutions give well-resolved spectra (Figure 5) with rhombic symmetry like that found for a wide variety of analogous metal bis(dithiolene) complexes.[1] The observed g-tensor components (Table IV) have been assigned by analogy with those determined[24] from single-crystal ESR measurements on $[Ni(mnt)_2]^-$ (mnt = maleonitriledithiolato), namely $g_1 = g_x$, $g_2 = g_y$, and $g_3 = g_z$, where g_1 and g_3 refer to the lowest and highest field g values, respectively:

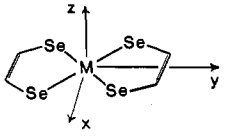

Comparison of the $[Ni(tds)_2]^-$ and $[Pt(tds)_2]^-$ g values with those

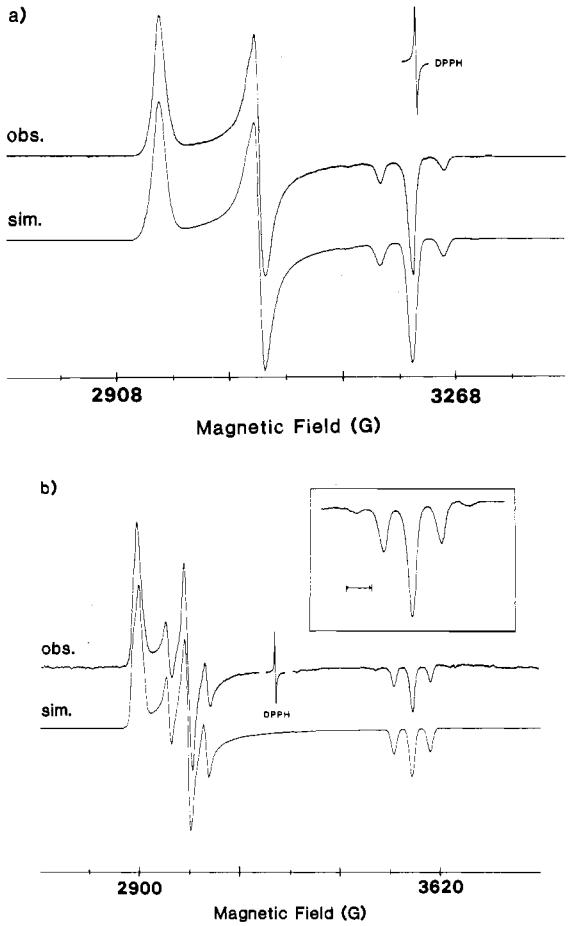

Figure 5. X-Band (9.045-GHz) ESR spectra of (a) $[Ni(tds)_2]^-$ and (b) $[Pt(tds)_2]^-$ in toluene–acetone (1:1) glasses at 77 K. The inset in (b) shows details of hyperfine structure on g_z; fiduciary marks represent 40 G. Simulated spectra were obtained by using the spin-Hamiltonian parameters listed in Table IV.

Table IV. ESR Parameters for $[M(tds)_2]^-$ (M = Ni, Pt) Anions and Comparable Metal Bis(dithiolene) Anions[a]

complex		*x*	*y*	*z*	ref
$[Ni(tds)_2]^-$	*g*	2.188	2.112	2.006	*c*
	A^{Se}	61	51	190	
$[Ni(tfd)_2]^-$	*g*	2.137	2.043	1.996	10b
$[Ni(mnt)_2]^-$	*g*	2.140	2.043	1.996	*d*
$[Pt(tds)_2]^-$	*g*	2.230	2.143	1.820	*c*
	A^{Se}	70	50	220	
	A^{Pt}	70	270	225	
$[Pt(tfd)_2]^-$	*g*	2.210	2.074	1.823	10b
	A^{Pt}	≤20	361	330	
$[Pt(mnt)_2]^-$	*g*	2.221	2.067	1.825	*d*, *e*
	A^{Pt}[b]	0	376	297	

[a] Data from low-temperature solution spectra unless otherwise noted. Hyperfine parameters are given in MHz. [b] Single-crystal data. [c] This work. [d] Davison, A.; Edelstein, N.; Holm, R. H.; Maki, A. H. *J. Am. Chem. Soc.* **1963**, *85*, 2029–2030. [e] Kirmse, R.; Dietzsch, W.; Solovĕv, B. V. *J. Inorg. Nucl. Chem.* **1977**, *39*, 1157–1160.

(24) Maki, A. H.; Edelstein, N.; Davison, A.; Holm, R. H. *J. Am. Chem. Soc.* **1964**, *86*, 4580–4587.

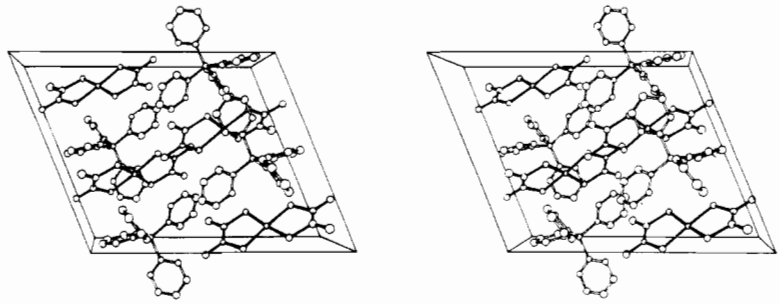

Figure 6. Stereoview of the molecular packing within the $[(C_6H_5)_4P][Pt(tds)_2]$ unit cell. The *a* axis is horizontal; *b* is into the page. The anions are highlighted with shaded bonds; F and H atoms have been omitted for clarity.

of the analogous $[M(tfd)_2]^-$ and $[M(mnt)_2]^-$ complexes given in Table IV reveals a pronounced shift in g_y upon substituting selenium for sulfur; although this shift might reflect in part the influence of the larger spin–orbit coupling[25] of the heavier chalcogen atoms, it is more likely to result from differences in the pattern of molecular orbital energies.

The low-temperature spectra of both $[Pt(tds)_2]^-$ and $[Ni(tds)_2]^-$ also show rich hyperfine structure arising from coupling of the unpaired electron spin with ^{195}Pt ($I = {}^1/_2$; 33.8%) and the four equivalent ^{77}Se nuclei ($I = {}^1/_2$; 7.58%); these couplings have been assigned on the basis of the results of computer spin simulations (Figure 5; Table IV). For example, we find that the spectrum of $[Pt(tds)_2]^-$ exhibits ^{195}Pt splittings on all three **g**-tensor components; as shown in Table IV, the analogous bis(dithiolene) complex $[Pt(tfd)_2]^-$ shows a qualitatively similar pattern of ^{195}Pt splittings (i.e., $A_y > A_z \gg A_x$), but the couplings are significantly larger. This comparison suggests that both complexes have similar electronic structures but that more spin density resides on Pt in the sulfur-based complex. In addition, the resolved ^{77}Se hyperfine splittings in the spectra of both $[Ni(tds)_2]^-$ and $[Pt(tds)_2]^-$ indicate extensive delocalization of the unpaired electron onto the ligands. Similar hyperfine structure from ^{33}S ($I = {}^1/_2$, natural abundance 0.79%) has been observed in frozen-solution spectra of several nickel bis(dithiolene) complexes.[26]

The spin-Hamiltonian parameters for the $[M(tds)_2]^-$ complexes given in Table IV indicate that, as with the corresponding metal bis(dithiolene) complexes,[27] the unpaired electron resides in a highly delocalized molecular orbital with B_{3g} symmetry (in D_{2h}), composed primarily of metal d_{yz} and selenium $4p_z$ orbitals:

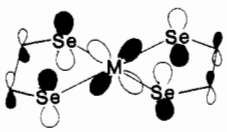

We can estimate the spin density residing on the selenium atoms in these complexes from the anisotropic component of the ^{77}Se hyperfine coupling (Table IV). A^{Se} is essentially axial, as expected for an electron in the $4p_z$ orbital; we ignore small deviations that arise from hybridization and take $A_\parallel^{Se} = A_z^{Se}$ and $A_\perp^{Se} = {}^1/_2(A_x^{Se} + A_y^{Se})$. The hyperfine splittings then can be written as $A_\parallel^{Se} = a + 2T$ and $A_\perp^{Se} = a - T$, where a is the isotropic contact term and T is the anisotropic dipolar term.[28] The approximate unpaired electron population per selenium atom is given by the ratio of the anisotropic hyperfine parameter T to the value $T_0^{Se} = 492$ MHz calculated[29] for the electron–nuclear interaction of a full electron in a ^{77}Se 4p orbital:

$$|C_{4p_z}|^2 = \rho_{spin} \simeq T/T_0^{Se} \qquad (3)$$

The experimentally derived values of T (and a) depend upon the relative signs of $A_\parallel$ and $A_\perp$ (i.e., the same or opposite). In principle, this could be determined from solution spectra since $\langle a \rangle = (A_\parallel + 2A_\perp)/3$; however, peak-to-peak line widths of 25 G (M = Ni) and 80 G (M = Pt) preclude the observation of resolved hyperfine splittings in solution.[30] Thus, we calculate T for both possibilities and choose the physically most reasonable result.

If $A_\perp$ and $A_\parallel$ have the same sign, the observed hyperfine splittings given in Table IV yield the values $T = 45$ and 53 MHz for M = Ni and Pt, respectively. Inserting these values into eq 3 yields spin densities of 0.09 (M = Ni) and 0.11 (M = Pt) per Se atom. Since there are four selenium atoms in each complex, this assignment suggests that ca. 40% of the total spin density in the HOMO of the paramagnetic monoanions resides on the chalcogen atoms, lower than the 50–65% obtained from both calculations[31] and experiment[26] for comparable metal bis(dithiolene) complexes. Alternatively, if $A_\perp$ and $A_\parallel$ have opposite signs, $T = 82$ MHz (M = Ni) and 93 MHz (M = Pt), corresponding to spin densities of 0.17 and 0.19 per Se, respectively. This assignment suggests that ca. 70% of the net spin density resides on the chalcogen atoms, a figure slightly higher than that found for the analogous sulfur complexes. The following arguments lead us to prefer the larger value for the spin density on selenium.

The narrow lines (full width at half height $\sim$10 G) indicate that there is little hyperfine coupling of the unpaired electron spin to the 12 ^{19}F ($I = {}^1/_2$, 100%) nuclei of the CF_3 substituents. Since the ESR lines would be broadened by β coupling to fluorine if the orbital coefficients of the carbon atoms in the chelate rings were large,[32] we infer that the spin density in the delocalized HOMO resides almost exclusively on the M–Se_4 core. For M = Pt, an independent measure of the spin density on the central metal ion can be obtained from a consideration of the ^{195}Pt hyperfine splittings. For the appropriate d_{yz} ground state, we follow Maki et al.[24,33] in relating this observed g and A^{Pt} values to the bonding parameter $T = \rho_{Pt}T_0^{Pt}$, where ρ_{Pt} is the spin density on platinum and $T_0^{Pt} = g_e\beta_e g_N\beta_N\langle r^{-3}\rangle \simeq 4.7 \times 10^{-2}$ cm^{-1}.[34] The

(25) Gordy, W. *Theory and Applications of Electron Spin Resonance*; Wiley-Interscience: New York, 1980; p 604.
(26) (a) Schmitt, R. D.; Maki, A. H. *J. Am. Chem. Soc.* **1968**, *90*, 2288–2292. (b) Kirmse, R.; Stach, J.; Dietzsch, W.; Steimecke, G.; Hoyer, E. *Inorg. Chem.* **1980**, *19*, 2979–2985.
(27) Alvarez, S.; Vicente, R.; Hoffmann, R. *J. Am. Chem. Soc.* **1985**, *107*, 6253–6277 and references therein.
(28) Wertz, J. E.; Bolton, J. R. *Electron Spin Resonance: Elementary Theory and Practical Applications*; McGraw-Hill: New York, 1972.
(29) Hurd, C. M.; Coodin, P. *J. Phys. Chem. Solids* **1967**, *28*, 523–525.
(30) Taking $A_\parallel$ and $A_\perp$ to have the same sign, we calculate $\langle a \rangle = 36$ and 40.5 G for Ni and Pt, respectively. While the value of 36 G for M = Ni is larger than the observed line width (25 G), it is probably not large enough to be resolved given the modest natural abundance (7.58%) of ^{77}Se. If $A_\parallel$ and $A_\perp$ have opposite signs, the calculated values $\langle a \rangle = 9.3$ G (M = Ni) and 12 G (M = Pt) are much smaller than the observed line widths.
(31) Sano, M.; Adachi, H.; Yamatera, H. *Bull. Chem. Soc. Jpn.* **1981**, *54*, 2636–2641.
(32) Reference 25, pp 272–276.
(33) We employ the equations given by Maki et al.[24]

$$g_{xx} = 2 - 6C_1 - 2C_3 \qquad g_{yy} = 2 - 2C_4 \qquad g_{zz} = 2 - 2C_2$$

$$A_{xx} = P[-6C_1 - 2C_3 - \kappa - 4/7 - 3C_2/7]$$

$$A_{yy} = P[-2C_4 - \kappa + 2/7 + (3/7)(C_1 + C_2 - C_3)]$$

$$A_{zz} = P[-2C_2 - \kappa + 2/7 + (3/7)(C_3 - C_1)]$$

where the various parameters are as defined in ref 24 and minor sign errors have been corrected.
(34) This value of T_0^{Pt} was calculated by using the value of $\langle r^{-3}\rangle = 12$ au for Pt^{3+}, given by: Simanek, E.; Sroubek, Z.; Zdansky, K.; Kaczes, J.; Novak, A. *Phys. Status Solidi* **1966**, *14*, 333–335.

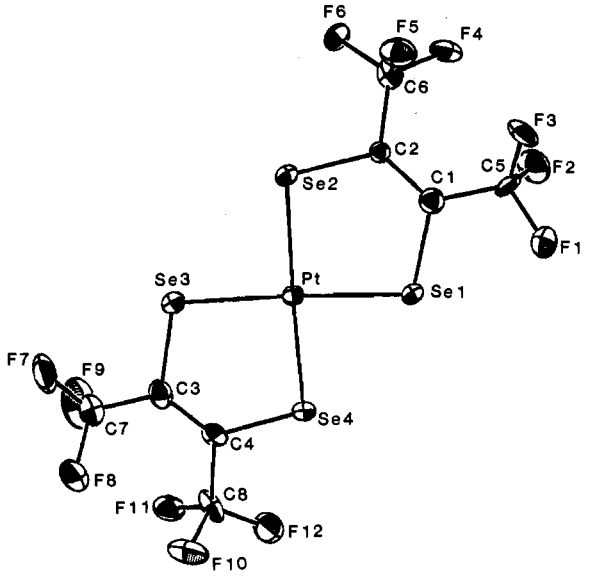

Figure 7. ORTEP plot of the $[Pt(tds)_2]^-$ anion viewed perpendicular to the molecular plane, showing the atom-numbering scheme. Atoms are drawn as 50% probability thermal ellipsoids.

^{195}Pt hyperfine tensor is approximately axial ($A_\parallel^{Pt} = A_x$), and again there are two possible assignments for the relative signs of $A_\parallel^{Pt}$ and $A_\perp^{Pt}$. For $A_\parallel^{Pt}$ and $A_\perp^{Pt}$ of the same sign, $T = 7.9 \times 10^{-3}$ cm^{-1} and $\rho_{Pt} = 0.17$, while for opposite signs, $T = 1.3 \times 10^{-2}$ cm^{-1} and $\rho_{Pt} = 0.28$. In either case *at most* ca. 30% of the spin density resides on the metal, which leads us to favor the larger value, $\rho_{Se} = 0.19$, because the other possibility, with $\rho_{Se} = 0.11$, would place unreasonably large spin densities on the ethylene carbons.

Crystal Structure of $[(C_6H_5)_4P][Pt(tds)_2]$. Crystals of $[(C_6H_5)_4P][Pt(tds)_2]$ are monoclinic, space group $P2_1/c$. A stereoscopic view of the molecular packing within the unit cell is shown in Figure 6. The $[Pt(tds)_2]^-$ anions are arranged in pairs about the symmetry centers at 0, 0, 0 and 0 $^1/_2$, $^1/_2$; the molecular planes of each pair of anions are therefore constrained to be parallel, but they do not overlap. The shortest Pt···Pt distance is 8.192 (2) Å, while the shortest interanion contact is 4.134 (4) Å, between Se atoms. The latter value is larger than the 4.0-Å van der Waals contact distance[35] for Se, and thus there appear to be no strong interactions within the anion pairs. Neighboring pairs of $[Pt(tds)_2]^-$ anions are separated by the phenyl substituents of the surrounding $[(C_6H_5)_4P]^+$ cations. The shortest anion–cation contact is 3.10 (2) Å, F(1)–C(23) and F(7)–C(13), less than the van der Waals contact distance of ca. 3.17 Å.

A similar crystal-packing motif is found in the related metal bis(dithiolene) salt $[PCl(C_6H_5)_3][Au(tfd)_2]$.[36] Here, too, the structure consists of well-separated pairs of complex anions arranged about symmetry centers, but in this case there is substantial overlap between the parallel molecular planes within the pairs. The Au···Au distance is 4.66 Å, and the shortest interanion contact (3.96 Å) is of the Au···S, rather than S···S, type. The different character of the intermolecular contacts within the anion pairs in the two structures apparently is determined by the different steric requirements of the $[PCl(C_6H_5)_3]^+$ and $[(C_6H_5)_4P]^+$ cations.

The structure of the $[Pt(tds)_2]^-$ anion (Figure 7; Table V) is similar to that found[37] for the analogous $[Pt(tfd)_2]^-$ complex. The coordination of the Pt atom is approximately square planar. The Se atoms exhibit a slight D_{2d} ruffling, with deviations (Å) from the least-squares plane defined by the $PtSe_4$ core as follows: Se(1), −0.108; Se(2), +0.108; Se(3), −0.104; Se(4), +0.111. There is also a slight distortion within the plane that is reflected in the different values of the two interligand Se–Pt–Se angles (88.28 (7) and 91.63 (7)°). The average Pt–Se bond distance of 2.367 (2) Å falls just below the range of 2.376 (2)–2.590 (7) Å for reported Pt–Se bond lengths[38] and is ca. 0.08 Å less than the sum of the Pauling covalent radii for Pt and Se. This suggests that the Pt–Se bonds in this complex have appreciable multiple-bond character. The analogous diselenocarbamate complex $[Pt(Se_2CN(t\text{-}C_4H_9)_2)_2]$[38e] has a significantly longer average Pt–Se bond distance of 2.428 (3) Å, which presumably is associated with the smaller internal Se–Pt–Se angle, 77.8 (1)°, in this complex.

As indicated in Table VI, the metrical parameters of the ligands in the $[Pt(tds)_2]^-$ ion are similar to those found in the analogous $[Ni(tds)_2]^-$ ion[9b] and the related trigonal-prismatic complex $[Mo(tds)_3]$.[39] For example, the average Se–C bond length of 1.88 (2) Å and the average C=C bond length of 1.37 (2) Å are both identical, within experimental error, to those of the Mo and

Table V. Selected Bond Distances (Å) and Angles (deg)

Pt–Se(1)	2.360 (2)	C(2)–C(6)	1.53 (2)
Pt–Se(2)	2.370 (2)	F(1)–C(5)	1.32 (2)
Pt–Se(3)	2.371 (2)	F(2)–C(5)	1.35 (2)
Pt–Se(4)	2.365 (2)	F(3)–C(5)	1.31 (2)
Se(1)–C(1)	1.87 (2)	F(4)–C(6)	1.36 (2)
Se(2)–C(2)	1.88 (2)	F(5)–C(6)	1.33 (3)
Se(3)–C(3)	1.90 (2)	F(6)–C(6)	1.32 (2)
Se(4)–C(4)	1.88 (2)	F(7)–C(7)	1.35 (2)
C(1)–C(2)	1.38 (2)	F(8)–C(7)	1.38 (2)
C(1)–C(5)	1.50 (3)	F(9)–C(7)	1.30 (3)
C(3)–C(4)	1.36 (3)	F(10)–C(8)	1.34 (2)
C(3)–C(7)	1.45 (3)	F(11)–C(8)	1.36 (3)
C(4)–C(8)	1.53 (2)	F(12)–C(8)	1.32 (2)
Se(1)–Pt–Se(2)	90.24 (7)	Se(2)–C(2)–C(1)	123 (1)
Se(1)–Pt–Se(4)	88.27 (7)	Se(2)–C(2)–C(6)	112 (1)
Se(2)–Pt–Se(3)	91.64 (7)	Se(3)–C(3)–C(4)	120 (2)
Se(3)–Pt–Se(4)	90.33 (7)	Se(3)–C(3)–C(7)	114 (1)
Pt–Se(2)–C(2)	102.3 (4)	Se(4)–C(4)–C(3)	124 (1)
Pt–Se(1)–C(1)	104 (6)	Se(4)–C(4)–C(8)	111 (1)
Pt–Se(3)–C(3)	103.3 (6)	C(3)–C(4)–C(8)	125 (2)
Pt–Se(4)–C(4)	102.2 (5)	C(2)–C(1)–C(5)	126 (1)
Se(1)–C(1)–C(2)	120 (1)	C(1)–C(2)–C(6)	124 (2)
Se(1)–C(1)–C(5)	114 (1)	C(4)–C(3)–C(7)	126 (2)

Table VI. Average Bond Distances (Å), Angles (deg), and Nonbonding Contacts (Å) for $M(tds)_x$ Complexes[a]

	$[Pt(tds)_2]^-$	$[Mo(tds)_3]$	$[Ni(tds)_2]^-$
	Bond Distances		
M-Se	2.367 (2)	2.492 (2)	2.255 (3)
Se–C	1.88 (2)	1.87 (1)	1.88 (1)
C=C	1.37 (2)	1.38 (2)	1.35 (2)
C—C	1.50 (2)	1.53 (2)	1.47 (2)
C—F	1.34 (2)	1.26 (2)	1.28 (2)
	Bond Angles[b]		
Se—M—Se	90.29 (7)	83.4 (1)	92.4 (1)
Se—M—Se′	89.96 (7)	80.5 (1)	87.6 (1)
Se—C=C	122 (1)	121.2 (4)	121 (1)
Se—C—C(F_3)	113 (1)	112 (1)	115 (1)
	Nonbonding Contacts[b]		
Se···Se	3.345 (3)	3.317 (5)	3.256 (6)
Se···Se′	3.356 (3)	3.222 (3)	3.121 (5)

[a] $[Mo(tds)_3]$ data from ref 35; $[Ni(tds)_2]^-$ data from ref 9b, room-temperature structure. [b] Se atoms belonging to different ligands are indicated with primes; i.e., Se—M—Se′ is an interligand angle.

(35) Pauling, L. *The Nature of the Chemical Bond*, 3rd ed.; Cornell University Press: Ithaca, NY, 1960; p 260.
(36) Enemark, J. H.; Ibers, J. A. *Inorg. Chem.* **1968**, *7*, 2636–2642.
(37) Kasper, J. S.; Interrante, L. V. *Acta Crystallogr., Sect. B: Struct. Crystallogr. Cryst. Chem.* **1976**, *B32*, 2914–2916.
(38) (a) Roesky, H. W.; Gries, T.; Hoffman, H.; Schimkowiak, J.; Jones, P. G.; Meyer-Base, K.; Sheldrick, G. M. *Chem. Ber.* **1986**, *119*, 366–373. (b) Chadha, R. K.; Chehayber, J. M.; Drake, J. E. *Inorg. Chem.* **1986**, *25*, 611–615. (c) Hope, E. G.; Levason, W.; Webster, M.; Murray, S. G. *J. Chem. Soc., Dalton Trans.* **1986**, 1003–1009. (d) Siedel, A. R.; Etter, M. C.; Jones, M. E.; Filipovich, G.; Mishmash, H. E.; Bahmet, W. *Inorg. Chem.* **1982**, *21*, 2624–2629. (e) Pan, W.-H.; Fackler, J. P.; Chen, H.-W. *Inorg. Chem.* **1981**, *20*, 856–863. (f) Chen, H.-W.; Fackler, J. P.; Masters, A. F.; Parr, W.-H. *Inorg. Chim. Acta* **1979**, *35*, L333. (g) Abel, E. W.; Kahn, R. A.; Kite, K.; Orrell, K. G.; Sik, V.; Cameron, T. S.; Cordes, R. *J. Chem. Soc., Chem. Commun.* **1979**, 713–714.
(39) Pierpont, C. G.; Eisenberg, R. *J. Chem. Soc. A* **1971**, 2285–2289.

Ni complexes. While the M-Se distances and internal Se-M-Se angles vary considerably within the series M = Pt, Ni, and Mo, the other angles within the five-membered metal-ligand chelate ring show relatively minor variations. The insensitivity of the ligand geometry to the size and/or coordination number of the central metal ion is highlighted by considering the nonbonding intramolecular Se···Se contacts. While the interligand Se···Se distances vary from 3.356 (3) to 3.121 (5) Å, the corresponding intraligand Se···Se distances, which reflect the chelate bite of the ligands, fall within the more limited range of 3.345 (3)-3.256 (6) Å. Thus, the tds ligands appear to adjust to different bonding situations by altering the M-Se distances while maintaining a relatively constant bite; the preferred ligand geometry apparently is determined by the importance of π-bonding in the highly delocalized electronic structures of these complexes.

Acknowledgment. We thank Dr. M. J. Natan for assistance with the electrochemical measurements. This work was supported by the Solid State Chemistry Program of the National Science Foundation (Grant DMR 85-19233 to B.M.H.); it benefited from the Northwestern University Materials Research Center under the NSF-MRL program (Grant DMR 85-20280). We further acknowledge Johnson Matthey Inc. for the loan of platinum salts.

Registry No. I (E = Se), 17744-01-3; $[(C_4H_9)_4N][Ni(tds)_2]$, 110304-00-2; $[(C_4H_9)_4N]_2[Ni(tds)_2]$, 113352-30-0; $[Ni(tds)_2]$, 28951-67-9; $[Cu(tds)_2]^-$, 47421-83-0; $[Cu(tds)_2]^{2-}$, 47451-04-7; $[Cu(tds)_2]$, 113378-58-8; $[(C_9H_5)_4P][Cu(tds)_2]$, 113352-38-8; $[Pt(tds)_2]^-$, 102764-51-2; $[Pt(tds)_2]^{2-}$, 113352-31-1; $[Pt(tds)_2]$, 113378-33-9; $[(C_6H_5)_4P][Pt(tds)_2]$, 113352-36-6; $[(C_6H_5)_4P]_2[Pt(tds)_2]$, 113352-37-7; $[(C_4H_9)_4N][Au(tds)_2]$, 113352-33-3; $[Au(tds)_2]^{2-}$, 113352-34-4; $[Au(tds)_2]$, 113352-35-5; $(Ph_3P)_2NiCO_2$, 13007-90-4; $(Ph_3P)_2PtCl_2$, 10199-34-5; $(Ph_3P)CuI$, 47107-74-4; $(Ph_3P)AlCl$, 14243-64-2.

Supplementary Material Available: Listings of all distances and angles, hydrogen atom parameters, and temperature factors (4 pages); a listing of calculated and observed structure factors (33 pages). Ordering information is given on any current masthead page.

Contribution from the Department of Chemistry,
State University of New York, Buffalo, New York 14214

Electrochemistry of Molybdenum Chloride Dimers in a Basic Ambient-Temperature Molten Salt

Richard T. Carlin and Robert A. Osteryoung*

Received August 6, 1987

The molybdenum(III) dimers $Mo_2Cl_9^{3-}$ and $Mo_2Cl_8H^{3-}$ and the molybdenum(II) dimer $Mo_2Cl_8^{4-}$ have been studied in the basic ambient-temperature molten salt $AlCl_3$-1-methyl-3-ethylimidazolium chloride (ImCl) by employing electrochemistry and visible spectroscopy. Both Mo(III) dimers are reduced to the Mo(II) dimer at approximately the same potential in a single, irreversible, two-electron step. The quadruply bonded dimer, $Mo_2Cl_8^{4-}$, undergoes a quasi-reversible, one-electron oxidation to $Mo_2Cl_8^{3-}$ and is further oxidized to $Mo_2Cl_9^{3-}$ in an irreversible, one-electron step at a more anodic potential. The hydride dimer $Mo_2Cl_8H^{3-}$ undergoes an irreversible, two-electron oxidation that produces $Mo_2Cl_9^{3-}$ and a proton. The electrochemical and chemical interconversions of the dimers are summarized as follows:

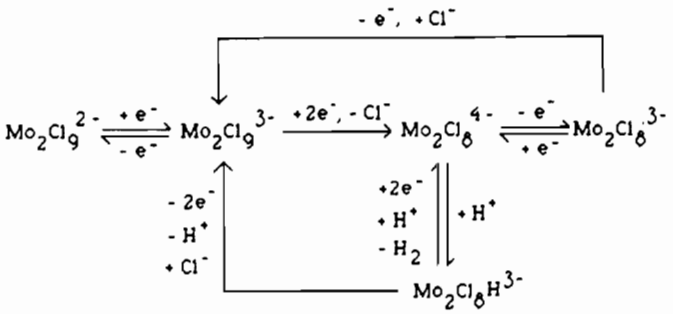

Introduction

Mixtures of $AlCl_3$ and 1-methyl-3-ethylimidazolium chloride (ImCl) form molten salts that remain liquid at ambient temperatures over a wide range of compositions.[1] Compositions with $AlCl_3$:ImCl molar ratios <1.0 are termed basic since chloride ion, a weak Lewis acid, is in excess, and the dominant anion species are chloride and tetrachloroaluminate, $AlCl_4^-$. Compositions with $AlCl_3$:ImCl molar ratios >1.0 are termed acidic, since excess $AlCl_3$ results in the formation of the strong Lewis acid $Al_2Cl_7^-$, and the dominant anion species are $Al_2Cl_7^-$ and $AlCl_4^-$. The wide electrochemical windows available in these molten salts make them attractive solvents for electrochemical examination of both inorganic and organic species.[1] In the basic melt, the anodic limit is determined by chloride oxidation, and the cathodic limit is set by reduction of the imidazolium cation. In the acidic melt, the anodic limit is determined by the oxidation of the $AlCl_4^-$ anion, and the cathodic limit is set by reduction of the $Al_2Cl_7^-$ anion to Al metal.[1]

In group VIa, both molybdenum and tungsten chloride complexes have been studies in the basic 0.8:1.0 $AlCl_3$:ImCl melt. Hexachloromolybdate monomers were found to exhibit a quasi-reversible Mo(III)/Mo(IV) redox couple.[2] In the case of tungsten, both the hexachlorotungstate monomers and the nonachloroditungstate(III) dimer, $W_2Cl_9^{3-}$, have been studied.[3] The hexachlorotungstate monomeric species exhibited two quasi-reversible redox couples, a W(III)/W(IV) couple and a W(IV)/W(V) couple. The electrochemistry of the tungsten dimer was more complex and involved dissociation into monomeric species.[3]

To extend the electrochemical studies of the group VIa metals, we undertook a study of the molybdenum dimer species $Mo_2Cl_9^{3-}$, $Mo_2Cl_8H^{3-}$, and $Mo_2Cl_8^{4-}$ in the basic melt. In the first two

(1) Hussey, C. L. In *Advances in Molten Salt Chemistry*; Mamantov, G., Ed.; Elsevier: Amsterdam, 1983; Vol. 5, pp 185-229.

(2) Scheffler, T. B.; Hussey, C. L.; Seddon, K. R.; C. M. Kear, C. M.; Armitage, P. D. *Inorg. Chem.* **1983**, *22*, 2099.

(3) Scheffler, T. B.; Hussey, C. L. *Inorg. Chem.* **1984**, *23*, 1926.

0020-1669/88/1327-1482$01.50/0